LOW-TEMPERATURE GETTERING OF IRON IN MONO- AND MULTICRYSTALLINE SILICON

Rafael Krain, Sandra Herlufsen and Jan Schmidt
Institut für Solarenergieforschung Hameln (ISFH), Am Ohrberg 1, D-31860 Emmerthal, Germany
Tel: +49 5151 999 636, Fax: +49 5151 999 600, Email: r.krain@isfh.de

ABSTRACT: The interstitial iron (Fe_i) concentrations in multicrystalline block-cast silicon (mc-Si) and monocrystalline Czochralski-grown silicon (Cz-Si) wafers deduced from recombination lifetime measurements are effectively reduced by annealing the wafers at very low temperature (300-500°C). During annealing the iron concentration decreases exponentially by more than one order of magnitude. Our results suggest that iron precipitation in the silicon bulk is the main mechanism responsible for the reduction in the Fe_i concentration.

Keywords: Silicon, Iron, Recombination

1 INTRODUCTION

Iron is one of the most detrimental impurities in silicon wafers as used in the production of solar cells, especially in multicrystalline silicon (mc-Si) wafers. In block-cast mc-Si it is typically found that most iron is present in the form of precipitates attached to crystallographic defects such as dislocations and grain boundaries. Total iron concentrations reported in the literature, measured in typical mc-Si block-cast and ribbon-grown wafers by neutron activation analysis (NAA), are in the range between $1 \times 10^{14}\text{cm}^{-3}$ and $6 \times 10^{14}\text{cm}^{-3}$ [1-3]. Most of this iron has been shown to be present in the form of precipitates which are, however, much less effective recombination centres than isolated interstitial iron (Fe_i). In particular in regions of low crystallographic defect densities, the recombination lifetime in mc-Si is largely limited by iron in its interstitial form. Hence, in order to significantly improve the material quality in terms of recombination lifetime, a reduction of the Fe_i concentration would be beneficial. External gettering, such as segregation gettering during phosphorus diffusion, is frequently applied in solar cell fabrication processes to effectively reduce the interstitial iron concentration [4]. These gettering techniques typically require high temperatures (>800°C) [5,6]. We report on a low-temperature (300-500°C) alternative for silicon material based on an internal gettering mechanism that works without a high-temperature phosphorus diffusion. First results obtained on block-cast mc-Si wafers were already published in a recent contribution [7]. In this paper, we apply this low-temperature gettering process to mono- and multicrystalline silicon wafers and pin down the principal gettering mechanism.

2 EXPERIMENTAL DETAILS

We investigate block-cast mc-Si wafers with a specific resistivity of 0.8 Ωcm and a thickness of 225 µm and 5-Ωcm Cz-Si wafers with a thickness of 350 µm. All wafers are doped with boron. In order to reduce the surface recombination to a minimum, the samples are RCA-cleaned and both wafer surfaces are then passivated by means of remote plasma-enhanced-chemical-vapour-deposited silicon nitride films deposited at 400°C. This surface passivation provides very low surface recombination velocities <10 cm/s, allowing the identification of the measured effective lifetime with the bulk lifetime [8]. Lifetime measurements are performed using the quasi-steady-state photoconductance (QSSPC) technique (Sinton Consulting, WCT100) [9], which is capable of determining the lifetime of a silicon sample at a well-defined injection density. We use the QSSPC technique in order to extract the Fe_i concentrations as described in the following.

In equilibrium, the interstitial positively charged Fe_i in *p*-type silicon forms iron-boron (Fe_iB_s) pairs with the negatively charged substitional boron B_s. These pairs can be dissociated by energy supply, e.g. by illumination. Due to the different recombination parameters of Fe_i and Fe_iB_s pairs, different lifetimes are measured before and after dissociation of the Fe_iB_s pairs [10,11]. From the lifetimes measured in the associated and the dissociated state, it is hence possible to extract the interstitial iron concentration if the lifetime measurements are performed at a well-defined injection density as it is done in the case of the QSSPC technique. In this study, the associated state of the samples is realized by annealing the silicon wafers at 50°C for about 20 minutes on a hot-plate. Under these conditions each free Fe_i atom becomes bound to a B_s atom. The complete dissociation of the Fe_iB_s pairs ('dissociated state') is realized by illumination using a flash light of ~300 suns (decay time constant ~2 ms). We use a total number of 15 flashes to completely dissociate the Fe_iB_s pairs. The interstitial iron concentration $[Fe_i]$ is then calculated using the expression

$$[\mathrm{Fe_i}] = C(\Delta n, N_\mathrm{A})\left(\frac{1}{\tau_\mathrm{d}} - \frac{1}{\tau_\mathrm{a}}\right), \qquad (1)$$

where τ_a is the measured lifetime in the associated state, τ_d is the measured lifetime after complete dissociation and C is the calibration factor which is a function of the injection density Δn and the doping concentration N_A, calculated using the Shockley-Read-Hall theory [12,13] and the well-established energy levels and capture cross sections of Fe_i and Fe_iB_s [14]. The lifetime measurements in this study are performed in the injection density range between $\Delta n = 1 \times 10^{15}\text{cm}^{-3}$ and $3 \times 10^{15}\text{cm}^{-3}$ to avoid trapping effects, which dominate the lifetime at low injection levels [15].

3 MULTICRYSTALLINE SILICON

Five mc-Si samples from the same ingot are used to study the behaviour of interstitial iron in the bulk of the wafers during long-term annealing at low temperature (≤ 500°C). The samples are from different heights of one mc-Si ingot and hence have different interstitial iron

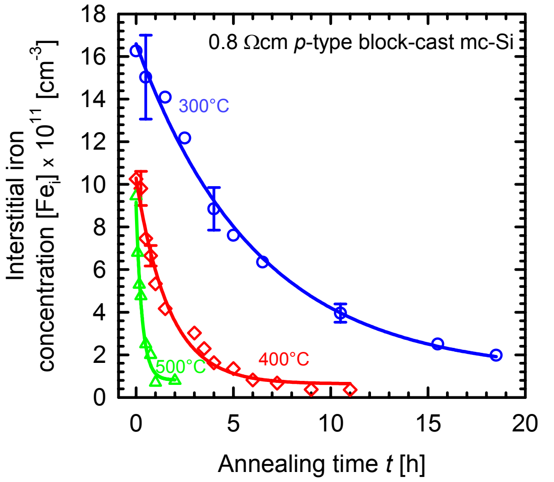

Figure 1: Evolution of the interstitial iron concentrations in mc-Si at 300, 400 and 500°C (symbols). The interstitial iron concentration is determined from lifetime measurements of the samples in the associated and dissociated state at an injection density of $\Delta n = 3 \times 10^{15}$cm^{-3}. The data are fitted by exponential decay functions (lines). From these fits the annealing time constants τ_{ann} are calculated for each temperature (see Tab. 1).

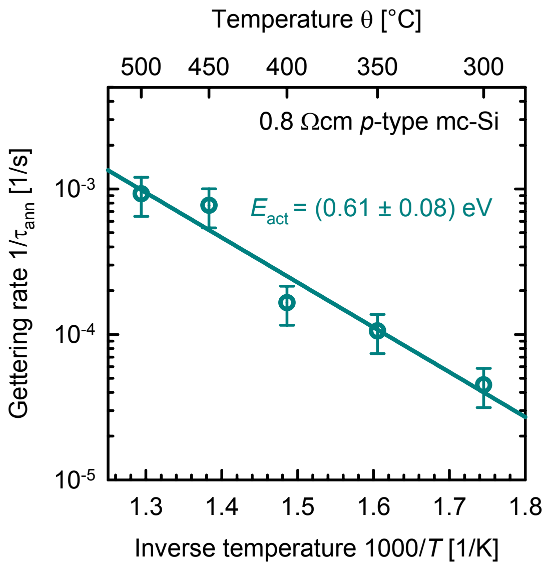

Figure 2: Experimentally determined rates $1/\tau_{ann}$ of the internal gettering process as a function of the inverse temperature in an Arrhenius plot. The calculated activation energy E_{act} for the gettering process is determined to $E_{act} = (0.61 \pm 0.08)$ eV.

concentrations before annealing. We anneal the samples at five different temperatures in the range between 300°C and 500°C. The carrier lifetimes are measured in the associated and dissociated states to determine the interstitial iron concentration using Eq. (1). The lifetimes of all samples are measured at an injection density of $\Delta n = 3 \times 10^{15}$cm^{-3}. Figure 1 shows exemplarily the evolution of the interstitial iron concentration at 300, 400, and 500°C. At all temperatures a surprisingly effective reduction of the interstitial iron concentration by more than one order of magnitude is achieved during the low-temperature annealing. The measured data points are fitted by an exponential decay function (lines). From these fits we determine the time constant τ_{ann} of the annealing process for each temperature. For increasing temperature the time constant decreases from 6.18 h at 300°C to 0.30 h at 500°C. The results of the measurements are summarised in Tab. 1. For samples A and C the determined interstitial iron concentration is reduced by one order of magnitude, and for samples B, D, and E the iron concentration decreases to below the detection limit of $[\mathrm{Fe_i}] \approx 1 \times 10^{10}$cm^{-3}. Consequently, for sample D and E, the interstitial iron concentration is reduced by at least two orders of magnitude. Note that a certain scattering in the measured iron concentration is expected from the fact that the QSSPC lifetime measurement technique detects the excess carrier concentration over an area of ~6 cm^2. As the defect distribution in mc-Si is typically very inhomogeneous, a certain scattering in the iron concentration is unavoidable, as only a small fraction of the total wafer area is covered by our measurement technique.

As can be seen from Tab. 1, the annealing time constant τ_{ann} strongly decreases with increasing annealing temperature, suggesting a thermally activated mechanism for the Fe$_i$ reduction. Figure 2 shows an Arrhenius plot of the inverse annealing time constant $1/\tau_{ann}$ as a function of the inverse annealing temperature $1/T$. The fact that the measured data can be well fitted by an Arrhenius law

$$\frac{1}{\tau_{ann}} = \nu \times \exp\left(-\frac{E_{act}}{kT}\right) \qquad (2)$$

verifies our above hypothesis of a thermally activated process.

The activation energy E_{act} is determined by means of a least-square fit of Eq. (2) to the measured data. This results in an activation energy of $E_{act} = (0.61 \pm 0.08)$ eV, which is close to the migration energy of interstitial iron in silicon $E_{mig.Fei} \approx (0.67 \pm 0.02)$ eV [16]. Our finding that $E_{act} \approx E_{mig.Fei}$ suggests that the migration of interstitial iron to gettering sites within the mc-Si wafer is the limiting mechanism in the Fe$_i$ removal process.

The observed effective reduction of Fe$_i$ in mc-Si may be explained by two different mechanisms. First, as mc-Si wafers have large numbers of crystallographic defects, in particular dislocations and grain boundaries, the Fe$_i$ could be gettered at these localized defect sites and regions of the wafer, which are virtually free from crystallographic defects, are effectively ‘cleaned’ by this internal gettering mechanism. This hypothesis is in agreement with the camera-based photoluminescence (PL) lifetime images [17,18] of an mc-Si sample (a) before and (b) after a long-term annealing treatment at 400°C as shown in Fig. 3. In regions with higher effective lifetimes before the thermal treatment, a significant increase of the effective lifetime can be observed after annealing, whereas regions with high crystallographic defect densities do not show any improvement. Second, we suggest that the iron forms iron silicide precipitates. In nearly defect-free monocrystalline float-zone silicon (FZ-Si) Henley and Ramappa [19] measured comparable annealing time constants (see also Fig. 6) for the interstitial iron reduction. They explained their experiments by temperature-dependent iron precipitation. The PL

Table 1: Summary of the data of the annealing experiments for each mc-Si wafer: Annealing temperatures θ, total durations *t* of the thermal treatments, annealing time constants τ_{ann} obtained from the fitted data and the interstitial iron concentrations before and after annealing are provided.

Sample	**Annealing Temperature θ** [°C]	**Total duration of thermal treatment *t*** [h]	**Annealing time constant τ_{ann}** [h]	**Interstitial iron concentration [Fe_i]** **before gettering** [cm^{-3}]	**after gettering** [cm^{-3}]
A	300	18.5	6.18	16.26×10^{11}	2.0×10^{11}
B	350	12	2.63	3.3×10^{11}	not detectable ($< 1 \times 10^{10}$)
C	400	11	1.68	10.3×10^{11}	0.4×10^{11}
D	450	4.5	0.36	3.9×10^{11}	not detectable ($< 1 \times 10^{10}$)
E	500	3.5	0.30	9.5×10^{11}	not detectable ($< 1 \times 10^{10}$)

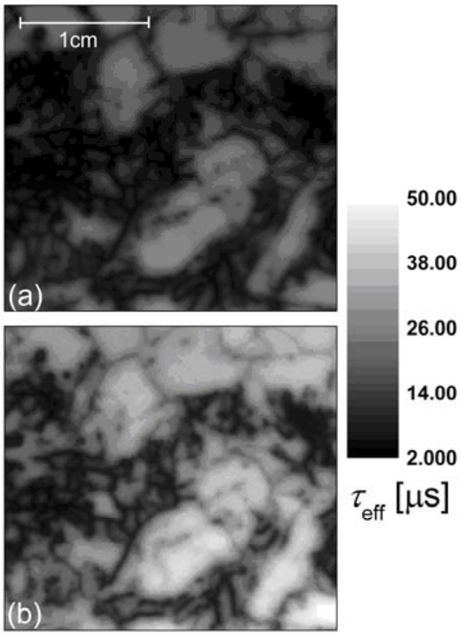

Figure 3: Photoluminescence lifetime images of an mc-Si wafer (a) before and (b) after long-term annealing at 400°C.

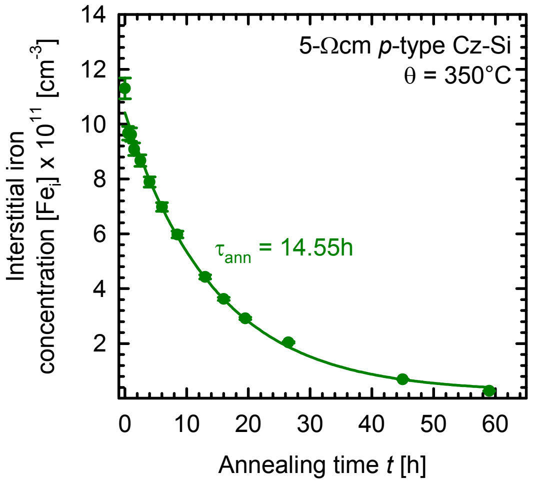

Figure 4: Evolution of the interstitial iron concentration in Cz-Si at 350°C. The data is fitted by an exponential decay function. The calculated annealing time constant is τ_{ann} = 14.55 h.

lifetime results shown in Fig. 3 are also fully consistent with the latter explanation which implies a homogeneous Fe_i reduction over the entire wafer. The lifetimes in the wafer regions with high crystallographic defect densities stay on a low level after gettering due to the large number of recombination centers not related to Fe_i concentration.

4 MONOCRYSTALLINE SILICON

We also applied the low-temperature gettering treatment to Cz-Si wafers contaminated with iron. Up to now, internal gettering has only been applied in microelectronics, where iron is gettered in the bulk of Cz-Si wafers by oxygen precipitates [20]. Fig. 4 shows the experimental results and the calculated annealing time constant at a temperature of 350°C. A pronounced reduction in the interstitial iron concentration of more than two orders of magnitude is observed.

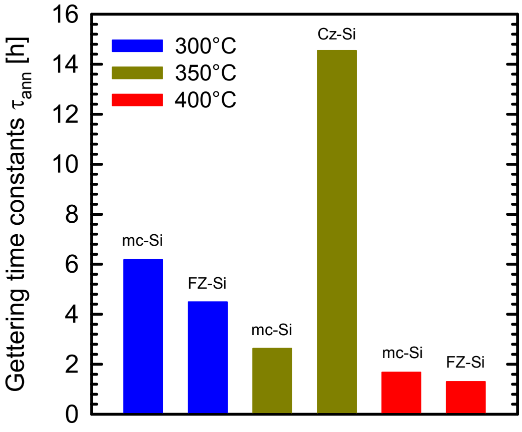

Figure 5: Comparison of the annealing time constants τ_{ann} at three different temperatures. The time constants of the mc-Si and FZ-Si are samples are comparable, while the Cz-Si time constant is much higher. The FZ-Si time constants are taken from the literature [19].

Figure 5 shows a comparison of the gettering time constants extracted for the different wafers. Also included are the data measured on FZ-Si wafers reported by Henley and Ramappa [19]. The time constants measured on FZ-Si are comparable to the time constants we extracted for mc-Si. These time constants are significantly below the time constants measured on the Cz-Si wafers. One major difference between Cz-Si and mc-Si is the much higher oxygen concentration in Cz-Si [21]. Our results suggest that the higher oxygen concentrations limit the diffusivity of the iron in Cz-Si, causing a slowing down of the internal gettering process.

The reduction of the Fe_i leads to a significant increase in the area-averaged lifetime. Figure 6 shows the comparison of the measured area-averaged lifetime before and after internal gettering at 350°C. In mc-Si the measured lifetime increases from 23 μs to 52 μs. In Cz-Si the lifetime increases from 27 μs to 280 μs.

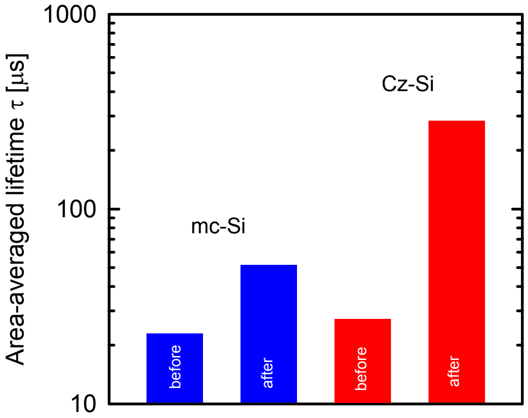

Figure 6: Comparison of the measured area-averaged lifetimes before and after internal gettering at 350°C. In mc-Si the lifetime nearly doubles. In Cz-Si the lifetime after gettering increases by one order of magnitude.

5 CONCLUSIONS

We have demonstrated the decrease of interstitial iron in multicrystalline and monocrystalline silicon by an internal gettering process at low temperatures (300-500°C). The interstitial iron concentration was found to decay exponentially by more than one order of magnitude. The Fe_i reduction mechanism was shown to be thermally activated and is characterised by an activation energy of $E_{act} = (0.61 \pm 0.08)$ eV, suggesting that the diffusion of Fe_i in silicon is the rate-limiting process. Comparison of our experimental results with literature data suggests that precipitation of iron is the predominant internal gettering mechanism.

In photovoltaics, internal gettering could open a way of further improving the quality of low-cost multicrystalline silicon. This low-temperature alternative works without a high-temperature phosphorus diffusion and is particularly relevant to low-temperature processed mc-Si solar cells, such as heterojunction cells. We have also studied the reversibility of the internal gettering mechanism up to a temperature of 600°C for 15 minutes. We found that no increase in the Fe_i concentration is observed after this additional annealing, leading to the conclusion that the internal gettering process is not reversible up to 600°C.

ACKNOWLEDGMENTS

The authors thank Daniel Macdonald (ANU) for valuable discussions. Funding was provided by the German State of Lower Saxony and the German Federal Ministry for the Environment, Nature Conservation, and Nuclear Safety (BMU) under Contract No. 0327650C.

REFERENCES

[1] A. A. Istratov, T. Buonassisi, R. J. McDonald, A. R. Smith, R. Schindler, J. A. Rand, J. P. Kalejs, and E. R. Weber, *J. Appl. Phys.* **94**, 6552 (2003).
[2] D. Macdonald, A. Cuevas, A. Kinomura, and Y. Nakano, *Proc. 29th IEEE PVSC*, New Orleans, USA (2002), p.285.
[3] D. Macdonald, A. Cuevas, A. Kinomura, Y. Nakano, and L. J. Geerlings, *J. Appl. Phys.* **97**, 033523 (2005).
[4] T. Buonassisi, M. D. Pickett, and R. Sweeney, *17th NREL Workshop on Crystalline Silicon Solar Cells and Modules: Materials and Processes*, Vail, CO (2007), p.218.
[5] J. Henze, P. Pohl, C. Schmiga, M. Dhamrin, T. Saitoh, I. Yamaga, and J. Schmidt, *20th EUPVSEC*, Barcelona, Spain (2005), p.769.
[6] J. Tan, A. Cuevas, D. Macdonald, T. Trupke, R. Bardos, and K. Roth, *Prog. Photovoltaics* **16**, 129 (2008).
[7] R. Krain, S. Herlufsen, and J. Schmidt, *Appl. Phys. Lett.* **93**, 152108 (2008).
[8] J. Schmidt and A. G. Aberle, *J. Appl. Phys.* **81** (9), 6186 (1997).
[9] R. A. Sinton and A. Cuevas, *Appl. Phys. Lett.* **69**, 2510 (1996).
[10] L. C. Kimerling and J. L. Benton, *Physica B & C* **116**, 297 (1983).
[11] G. Zoth and W. Bergholz, *J. Appl. Phys.* **67**, 6764 (1990).
[12] W. Shockley and W. T. Read, *Phys. Rev.* **87**, 835 (1952).
[13] R. N. Hall, *Phys. Rev.* **87**, 387 (1952).
[14] J. E. Birkholz, K. Bothe, D. Macdonald, and J. Schmidt, *J. Appl. Phys.* **97**, 103708 (2005).
[15] D. Macdonald and A. Cuevas, *Appl. Phys. Lett.* **74**, 1710 (1999).
[16] A. A. Istratov, H. Hieslmair, and E. R. Weber, *Appl. Phys. A* **69**, 13 (1999).
[17] T. Trupke, R. A. Bardos, M. C. Schubert, and W. Warta, *Appl. Phys. Lett.* **89**, 044107 (2006).
[18] S. Herlufsen, J. Schmidt, D. Hinken, K. Bothe, and R. Brendel, *Phys. Stat. Sol. (RRL)* **2**, 6, 245 (2008).
[19] W. B. Henley and D. A. Ramappa, *J. Appl. Phys.* **82**, 589 (1997).
[20] D. Gilles, E. R. Weber, and S. Hahn, *Phys. Rev. Lett.* **64** (2), 196 (1990).
[21] K. Bothe, R. Hezel, and J. Schmidt, *Sol. Stat. Phenom.* **95-96**, 223 (2004).